Desalination and Water Treatment
www.deswater.com

doi: 10.5004/dwt.2018.21912

104 (2018) 257–262
February

Separation and extraction of cesium from salt lake brine by the calcium alginate–ammonium tungstophosphate composite adsorbent

Tan Guo[a,*], Shan Yun[a], Lei He[a], Quan Li[b], Zhijian Wu[b]

[a]*Jiangsu Provincial Engineering Laboratory for Advanced Materials of Salt Chemical Industry, School of Chemical Engineering, Huaiyin Institute of Technology, No. 1 Meicheng Road, Huai'an 223003, China, Tel. +86 517 83559720; emails: guotan200613@126.com (T. Guo), yunshan@hyit.edu.cn (S. Yun), heleihuaian@hyit.edu.cn (L. He)*
[b]*Key Laboratory of Salt Lake Resources and Chemistry, Qinghai Institute of Salt Lakes, Chinese Academy of Sciences, No. 18 Xinning Road, Xining 810008, China, Tel. +86 971 6307871; emails: liquan@isl.ac.cn (Q. Li), zjwu@isl.ac.cn (Z. Wu)*

Received 12 June 2017; Accepted 11 January 2018

ABSTRACT

A composite adsorbent calcium alginate–ammonium tungstophosphate ($Ca(ALG)_2$–AWP) was synthesized by a sol-gel method using ammonium tungstophosphate ($(NH_4)_3PW_{12}O_{40}$) as the adsorption active component and calcium alginate ($Ca(ALG)_2$) as the matrix. Adsorption and desorption behaviors of Li^+, Na^+, K^+, Rb^+, Cs^+ and Mg^{2+} were investigated at 25°C comprehensively. Under competitive adsorption conditions, the separation factor was in the order of $\beta_{Cs/Mg} >> \beta_{Rb/Mg} > \beta_{Li/Mg} \sim \beta_{Na/Mg} \sim \beta_{K/Mg}$ explained by considering the hydration radius of metal ions, electrostatic attraction and Gibbs free energy. In the column tests, Cs^+ exhibited the lowest breakthrough ratio and highest selectivity. High quality of CsCl with the content of 82.44 wt% was obtained from the salt lake brine after desorption by the mixed solution of 3 mol L^{-1} NH_4Cl and 1 mol L^{-1} HCl. Therefore, the method of column adsorption–desorption by using $Ca(ALG)_2$–AWP was promising to separate and extract Cs^+ from the salt lake brine with high selectivity and excellent regeneration.

Keywords: Cesium; Adsorption; Desorption; Calcium alginate–ammonium tungstophosphate; Salt lake brine

1. Introduction

Rare metals such as Cs, which has special physical and chemical properties, play increasingly important roles in many fields such as production of scintillation counter [1], optical glass, atomic clocks [2], pharmaceuticals in medical treatment [3] and catalysts in chemical reaction [4,5], etc. The salt lakes in Qinghai Province and Tibet of China are abundant of Cs resource. However, the concentration of Cs^+ is extremely low (0.034 mg L^{-1} in Qaidam salt lake) in salt lake brine [6]. And Cs^+ coexists with Li^+, Na^+, K^+, Rb^+, Mg^{2+} and other ions which have similar physical and chemical properties with Cs^+ [7,8]. The concentration of these symbiotic metal ions was generally greater in several orders of magnitude than that of Cs^+. Thus, it is difficult to separate and extract Cs^+ from salt lake brine. Various methods including co-precipitation [9], solvent extraction [10] and adsorption [11–13] have been used for the separation of Cs^+. Among these methods, adsorption is an effective method to remove metal ions for water purification due to its advantages of easy operation, low energy consumption, high efficiency and inexpensive equipment [14–16]. Many adsorbents such as hexacyanoferrates [17,18], zeolite [19], heteropolyacids [20], crown ethers [21] and titanosilicates [22], etc., have been investigated to remove Cs^+ from the highly active liquid waste. Among these reported adsorbents, the heteropolyacids (e.g., ammonium tungstophosphate [AWP]) with efficient regenerating ability show a high selectivity toward Cs^+ [23,24]. However, AWP is not suitable for the practical separation–extraction process because of its fine powder form. Therefore, the granulation of AWP powder by alginate gel polymers has been one of the most prominent techniques for continuous treatment by the packed column.

* Corresponding author.

Herein we present the first example of the separation and extraction of cesium from salt lake brine by microencapsulated AWP. In this paper, a composite spherical adsorbent (calcium alginate [$Ca(ALG)_2$]–AWP) for cesium ions was synthesized using AWP as an adsorption active component and $Ca(ALG)_2$ as a carrier. The behaviors of adsorption and desorption of the typical coexistent ions Li^+, Na^+, K^+, Rb^+, Mg^{2+} and Cs^+ onto $Ca(ALG)_2$–AWP were investigated. And the solid compound of CsCl was successfully recovered from the salt lake brine by using the $Ca(ALG)_2$–AWP adsorbent with the content of 82.44 wt%.

2. Experimental setup

2.1. Reagents

The following chemicals were used in the synthesis of the composite adsorbent: AWP (Beijing Chemical Works, Beijing, China), sodium alginate (Sinopharm Chemical Reagent Co., Ltd., Shanghai, China) and calcium chloride (Tianjin Baishi Chemical Industry Co., Ltd., Tianjin, China). The concentrated salt lake brine samples (potassium was removed) were collected from Laguocuo playa in Tibet of China. The detailed compositions of the real brine (the residual salt lake brine) included Li^+ (23 g L^{-1}), Na^+ (24 g L^{-1}), K^+ (27 g L^{-1}), Rb^+ (0.85 g L^{-1}), Cs^+ (0.80 g L^{-1}), Mg^{2+} (20 g L^{-1}), Ca^{2+} (0.04 g L^{-1}), Sr^{2+} (0.0003 g L^{-1}), and small amounts of Fe, B, CO_3^{2-} and SO_4^{2-}.

2.2. Preparation of the composite adsorbent

A AWP ($(NH_4)_3PW_{12}O_{40}$) exchanger consisting of Keggin type [25] polyanions $PW_{12}O_{40}^{3-}$ and exchangeable NH_4^+ was used as the adsorption active component. The composite adsorbent of $Ca(ALG)_2$–AWP was prepared by a sol-gel procedure. 30 g AWP powder was dispersed into 150 mL of 2.5 wt% sodium alginate solution under vigorous stirring to get uniform suspensions. The suspensions were pumped dropwise into 300 mL 5 wt% $CaCl_2$ solution by a peristaltic pump to obtain composite gel beads. After 48 h aging, the gel beads were separated from the solution, successively washed with distilled water to remove Cl^-, and then stored in distilled water. These wet composite gel beads were used for the adsorption experiments.

2.3. Characterization methods

The water content of the wet composite adsorbent was measured using a MB45 moisture analyzer (Ohaus Corporation, Switzerland) heating at 90°C for 80 min. Scanning electron microscopy (SEM) images of the composite adsorbent were taken on a JSM-5610LV SEM instrument (JEOL Ltd., Japan). Before taking the SEM images, the adsorbent was dried at 25°C. The solid matters obtained from salt lake brine were characterized by energy dispersive spectroscopy (EDS) and X-ray diffraction (XRD). The EDS spectrum was performed using an INCA instrument (Oxford Instrument Co., Ltd., UK). The XRD pattern was collected on an X'Pert PRO diffractometer (PANalytical, Netherlands) using Cu K_α radiation (λ = 0.15419 nm) over a 2θ ranging from 5° to 70°.

2.4. Competitive adsorption experiments for the multi-element solution

The competitive adsorption experiments were performed by mixing 0.3 g wet $Ca(ALG)_2$–AWP adsorbent with 100 mL multi-element solution, where the concentration of each metal ion (Li^+, Na^+, K^+, Rb^+, Cs^+ and Mg^{2+}) was 0.01 mol L^{-1}, carried out at 25°C in a water bath (SHA-C, Changzhou Guohua Co., Ltd., China) with a shaking speed of 150 rpm.

The concentration of the metal ions was determined using an ICS-1100 ionic chromatograph (Dionex Corporation, USA). The adsorption amount of the metal ions onto the composite adsorbent was calculated by Eq. (1), where q (mmol·g^{-1}) is the adsorption amount of metal ions onto the $Ca(ALG)_2$–AWP at time t, V (L) is the volume of the multi-element solution, m (g) is the mass of the dry weight of the adsorbent, C_0 (mmol·L^{-1}) and C (mmol·L^{-1}) are metal ions concentration in multi-element solution at the beginning t_0 and time t, respectively. When the equilibrium solution concentration C_e was substituted for C, the equilibrium adsorption amount q_e was obtained.

$$q = \frac{V(C_0 - C)}{m} \tag{1}$$

2.5. Column experiments for salt lake brine

Column tests were carried out in the glass tube (inner diameter of 1.2 cm and length of 36 cm) densely filled with 20 g wet $Ca(ALG)_2$–AWP gel beads at 25°C. Salt lake brine as the feed solution was passed through the column at a constant flow rate of 0.55 mL min^{-1} by a peristaltic pump. During loading run, the effluent samples were collected periodically and analyzed by the ionic chromatograph. The breakthrough curves were obtained by plotting the breakthrough ratio (C/C_0) against the effluent volume (mL), where C_0 and C (mol·L^{-1}) are the concentrations of the initial feed solution and effluent, respectively. After saturation, the desorption of Cs^+ from adsorbents in the column was performed by using 3 mol L^{-1} NH_4Cl–1 mol L^{-1} HCl solution as an eluent. The flow rate of the eluent was maintained at 0.16 mL min^{-1}. The effluent was collected periodically and measured by ICS-1100, and the elution curve was obtained by plotting C (the concentration of Cs^+ in the effluent, mol·L^{-1}) against the effluent volume (mL). The above run was repeated for four cycles. The effluent solution of eluent was collected and then pretreated using an evaporation–crystallization technology. Then the pretreated solution was dried and calcined in a muffle furnace at 400°C for 4 h to gain the solid compound of CsCl. The technological process is described explicitly in Fig. 1.

3. Results and discussion

3.1. Characterization of $Ca(ALG)_2$–AWP

The average diameter of the wet $Ca(ALG)_2$–AWP beads is about 2 mm as shown in Fig. 2. The water content of the wet composite adsorbent was determined to be 67.72 wt%. SEM images of the dried $Ca(ALG)_2$–AWP beads are shown in Fig. 3. The surface morphology was uniform and the fine AWP crystals were well immobilized in the calcium alginate gel matrices.

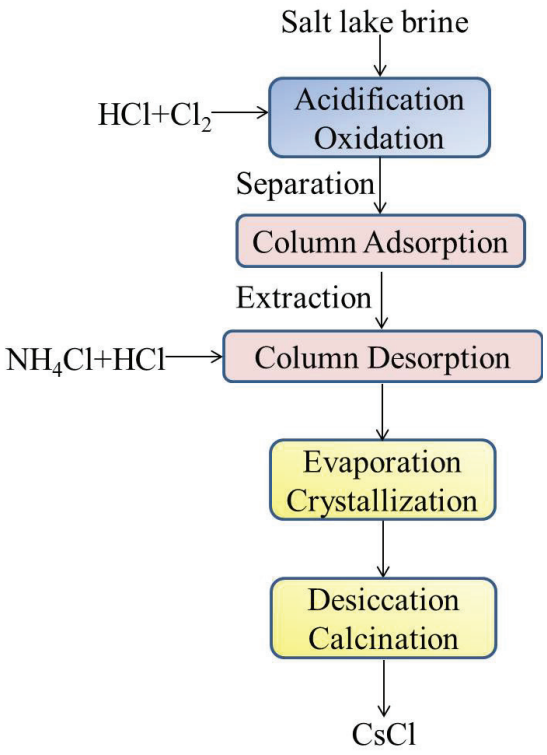

Fig. 1. Technological process of separation and extraction of Cs^+ from salt lake brine.

3.2. Adsorption kinetic curves for competitive conditions

As shown in Fig. 4(a), the uptake of Cs^+ is quickly increased during the initial 1 h, and the competitive adsorption reaches equilibrium after 2 h. The equilibrium adsorption amount was found to follow the order of Cs^+ >> Rb^+ > Li^+ ~ Na^+ ~ K^+ ~ Mg^{2+} and Li^+, Na^+, K^+, Mg^{2+} and Rb^+ were not easily adsorbed. In order to have a detailed comparison for the adsorption, separation factors (β) were calculated according to Eq. (2) based on the adsorption data at 2 h, where M denotes Li, Na, K, Rb or Cs, q_M is the equilibrium adsorption amount of metal ions onto the $Ca(ALG)_2$–AWP beads (mmol·g^{-1}), C_M is the equilibrium solution concentration of metal ions.

Fig. 2. Photograph of the $Ca(ALG)_2$–AWP beads.

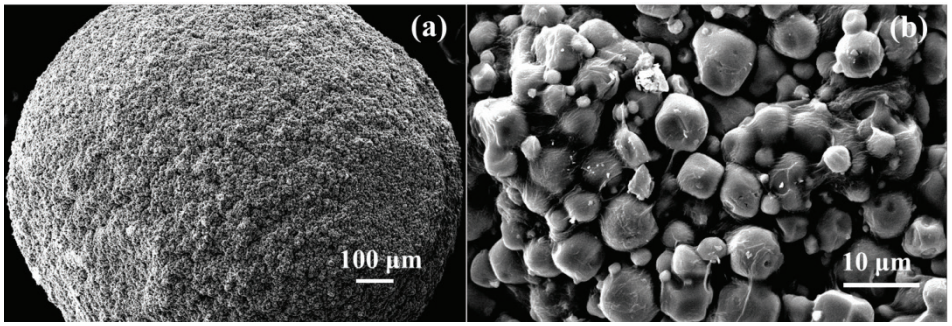

Fig. 3. SEM images of the $Ca(ALG)_2$–AWP beads. (a) ×100, (b) ×2,000.

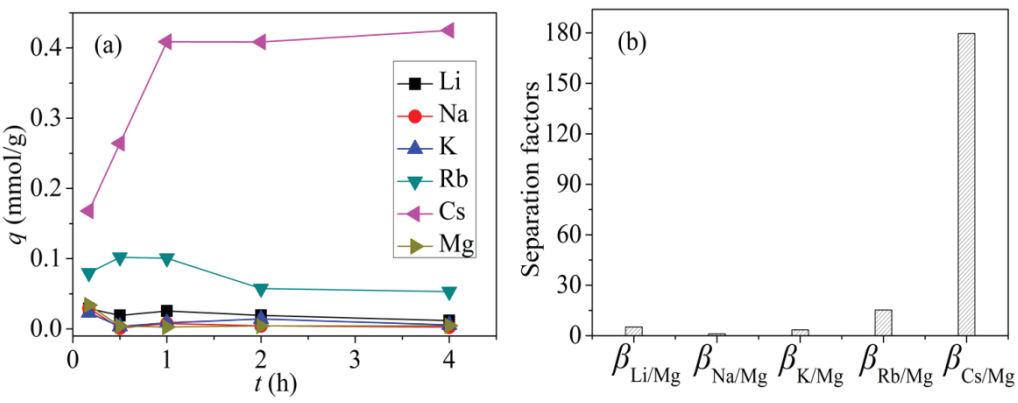

Fig. 4. Kinetic curves (a) and separation factors (b) for competitive adsorption.

$$\beta_{M/Mg} = (q_M/C_M)/(q_{Mg}/C_{Mg}) \quad (2)$$

The results are shown in Fig. 4(b) following the order of $\beta_{Cs/Mg} >> \beta_{Rb/Mg} > \beta_{Li/Mg} \sim \beta_{Na/Mg} \sim \beta_{K/Mg}$, which indicate that $Ca(ALG)_2$–AWP provides the superior selectivity toward Cs^+ over all other metal ions. The adsorption mechanism was proposed by the ion exchange reaction between Cs^+ and NH_4^+ expressed as Eq. (3):

$$Ca(ALG)_2–(NH_4)_3PW_{12}O_{40} + 3Cs^+ = Ca(ALG)_2–Cs_3PW_{12}O_{40} + 3NH_4^+ \quad (3)$$

The main reasons of the above results are summarized as follows: (1) the first one is probably that the hydration radius of Cs^+ (3.25 Å) just matches the channel diameter of $[PW_{12}O_{40}]^{3-}$ anions vacancy. The adsorption amount of the metal ions decreases with increasing the hydrated radii of the cations, namely, Cs^+ (3.25 Å) > Rb^+ (3.29 Å) > K^+ (3.31 Å) ~ Na^+ (3.58 Å) ~ Li^+ (3.82 Å) ~ Mg^{2+} (4.28 Å) [26]. (2) It may be demonstrated by the electrostatic attraction between metal ions and $[PW_{12}O_{40}]^{3-}$ anions. The hydrated radii of metal ions increasing gradually in the order of Cs^+ (3.25 Å) < Rb^+ (3.29 Å) < K^+ (3.31 Å) < Na^+ (3.58 Å) < Li^+ (3.82 Å) < Mg^{2+} (4.28 Å) [26–28], Cs^+ can reach to the adsorbent more closely, and therefore $[PW_{12}O_{40}]^{3-}$ anions show the highest affinity to Cs^+. (3) The relationship between the metal ions and adsorbent can be explained by adsorption reaction's Gibbs free energy (ΔG) [29] which is calculated by distribution coefficient (K_d) as Eqs. (4) and (5), and the results are listed in Table 1. The ΔG value of Cs^+ is considerably lower than those of other metal ions, indicating significantly higher selectivity for Cs^+ adsorption onto $Ca(ALG)_2$–AWP than those of Rb^+, Li^+, Na^+, K^+ and Mg^{2+}:

$$K_d = \frac{(C_0 - C_e)V}{mC_e} \quad (4)$$

$$\Delta G = -RT\ln K_d \quad (5)$$

3.3. Column adsorption and desorption behaviors for salt lake brine

The breakthrough curves of metal ions (salt lake brine as feed solution) for the four consecutive adsorption–desorption cycles are shown in Fig. 5. There was no obvious change in the breakpoint and the breakthrough capacity during 1st–4th adsorption cycles from Fig. 5. The breakthrough ratio (C/C_0) of Li^+, Na^+, K^+, Mg^{2+}, Cs^+ increased with increasing the effluent

Table 1
K_d and ΔG for metal ions adsorption onto $Ca(ALG)_2$–AWP at 25°C

Metal ions	K_d (mL·g^{-1})	ΔG (kJ·mol^{-1})
Li^+	0.499	1.72
Na^+	0.407	2.23
K^+	0.600	1.26
Rb^+	6.02	–4.45
Cs^+	83.2	–11.0
Mg^{2+}	0.455	1.95

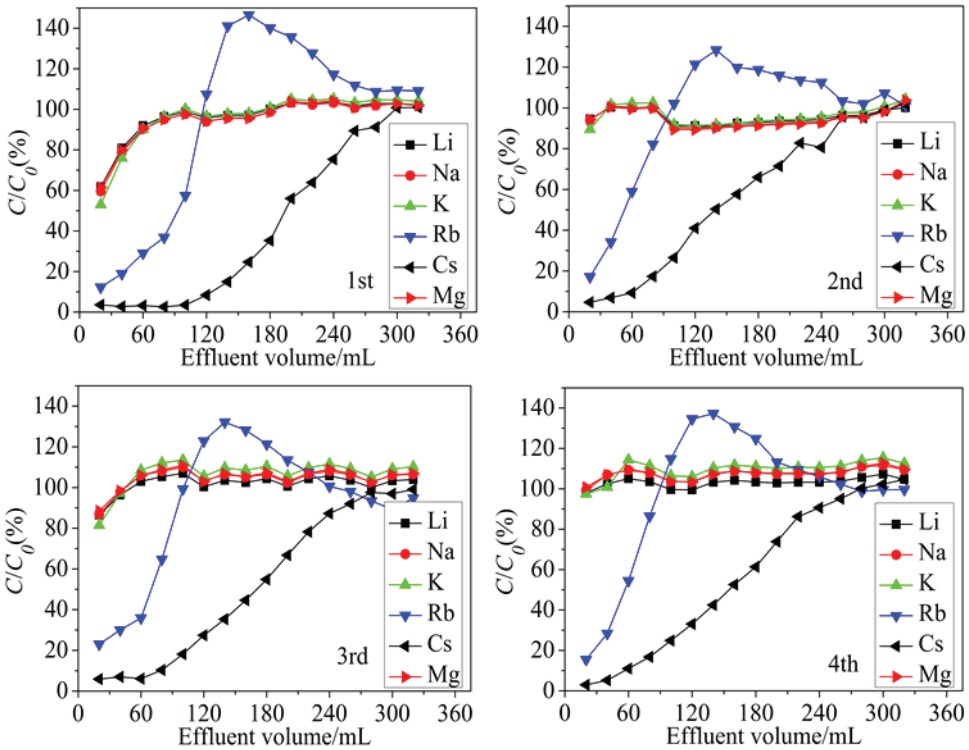

Fig. 5. Breakthrough curves of metal ions for repeated runs.

volume, which was caused by the increased concentration (C) of these metal ions in the effluent. The breakthrough ratio of Rb^+ at first increased to 120%–140% and then decreased to 100%, indicating that Rb^+ was firstly adsorbed onto the active sites of $Ca(ALG)_2$–AWP and then desorbed from the adsorbent. The lowest breakthrough ratio was obtained for Cs^+ adsorption. The column reached saturation after passing about 90 mL feed solution for Li^+, Na^+, K^+ and Mg^{2+}, 270 mL for Rb^+, and 300 mL for Cs^+. These results demonstrated that Li^+, Na^+, K^+, Mg^{2+} and Rb^+ were hardly adsorbed while Cs^+ was easily adsorbed in the column experiments. Thus, $Ca(ALG)_2$–AWP showed excellent performance for adsorptive separation of Cs^+ from salt lake brine.

Fig. 6 shows the elution curves of Cs^+ during the four consecutive adsorption–desorption cycles. The desorption amount of Cs^+ tended to decrease slightly with the increasing number of elution cycles, while the profiles of the four elution curves were almost same. Li^+, Na^+, K^+, Mg^{2+} and Rb^+ were not detectable in the effluent in the process of desorption. Cs^+ was completely desorbed from column with about 400 mL 3 mol L^{-1} NH_4Cl–1 mol L^{-1} HCl solution. Here the additional HCl was used to prevent the swelling of $Ca(ALG)_2$–AWP gel beads [24,30]. NH_4Cl–HCl solution has the advantage of simultaneous elution and regeneration of $Ca(ALG)_2$–AWP. In general, the method of column adsorption–desorption with the composite adsorbent of $Ca(ALG)_2$–AWP was proved to be effective for the selective uptake and recovery of Cs^+ from salt lake brine.

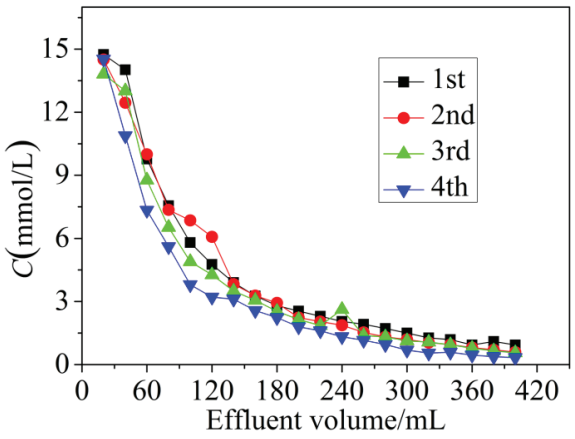

Fig. 6. Elution curves of Cs^+ for repeated runs.

The XRD and EDS patterns of the solid matter obtained from salt lake brine are shown in Figs. 7(a) and (b), respectively. Dominated CsCl phase with high intensity peaks was shown in Fig. 7(a). The major component of CsCl was further confirmed by the EDS patterns shown in Fig. 7(b). Minor elements of K and Na were also found in the EDS patterns. As determined by the ICS-1100 and listed in Table 2, CsCl was the main product with a high content of 82.44 wt%. These results are of great significance in providing guidance for extracting Cs^+ from the brine resources of salt lakes.

4. Conclusions

The composite adsorbent of $Ca(ALG)_2$–AWP gel beads was prepared by the sol-gel method. Under the competitive adsorption conditions, $Ca(ALG)_2$–AWP exhibited the highest selectivity for Cs^+ according to the value of q and β. In the column experiments, the lowest breakthrough ratio and highest selectivity were obtained for Cs^+, and the loaded Cs^+ onto the composite adsorbent was effectively desorbed by 3 mol L^{-1} NH_4Cl–1 mol L^{-1} HCl, which confirmed the composite adsorbent had excellent selectivity and efficient regeneration properties. The solid compound of CsCl with a content of 82.44 wt% can be obtained from the brine of salt lakes. During the 1st–4th absorption–desorption cycles, the adsorbent packed in the column showed stable performance on breakthrough and elution. The present column absorption–desorption technology is a promising approach for the separation and extraction of Cs^+ from the salt lake brine.

Table 2
Compositions of the solid matter obtained from salt lake brine

Salts	Weight %
LiCl	0.40
NaCl	9.29
KCl	1.54
RbCl	1.82
CsCl	82.44
$MgCl_2$	0.83
$CaCl_2$	2.46

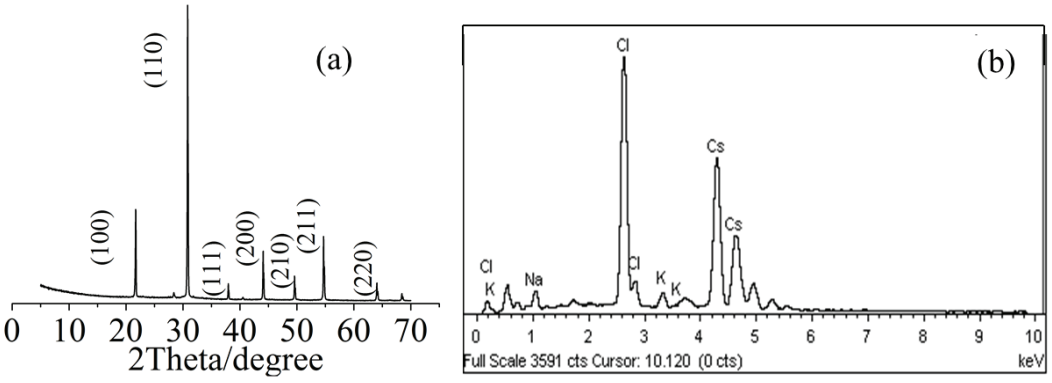

Fig. 7. XRD (a) and EDS (b) patterns of the solid matter obtained from salt lake brine.

Acknowledgements

This study was financially supported by Opening Funding of Jiangsu Provincial Engineering Laboratory for Advanced Materials of Salt Chemical Industry (contract No: SF201507), Natural Science Fund for Colleges and Universities in Jiangsu Province (contract No: 17KJB430004) and the Natural Science Foundation of Jiangsu Province (Grants No: BK20130420).

References

[1] F.L. Ruta, S. Swider, S. Lam, R.S. Feigelson, Understanding phase equilibria and segregation in Bridgman growth of Cs_2LiYCl_6 scintillator, J. Mater. Res., 32 (2017) 2373–2380.
[2] M.A. Hafiz, G. Coget, P. Yun, S. Guérandel, E. de Clercq, R. Boudot, A high-performance Raman-Ramsey Cs vapor cell atomic clock, J. Appl. Phys., 121 (2017) 104903–104912.
[3] B. Parashar, J. Port, S. Arora, P. Christos, S. Trichter, D. Nori, A.G. Wernicke, Analysis of stereotactic radiation vs. wedge resection vs. wedge resection plus cesium-131 brachytherapy in early stage lung cancer, Brachytherapy, 14 (2015) 648–654.
[4] Y. Kano, M.A. Ohshima, H. Kurokawa, H. Miura, Dehydrogenation of ethylbenzene over Fe-Ce-Rb and Fe-Ce-Cs mixed oxide catalysts, React. Kinet. Mech. Catal., 109 (2013) 29–41.
[5] G. Zhang, H. Zhang, D. Yang, C. Li, Z. Peng, S. Zhang, Catalysts, kinetics and process optimization for the synthesis of methyl acrylate over Cs-P/γ-Al_2O_3, Catal. Sci. Technol., 6 (2016) 6417–6430.
[6] S.M. Yan, J.Q. Sun, Assessing China's salt lake resources R&D based on bibliometrics analysis, Scientometrics, 105 (2015) 1141–1155.
[7] C. Sun, F. Zhang, J. Cao, A 'build-bottle-around-ship' method to encapsulate ammonium molybdophosphate in zeolite Y. An efficient adsorbent for cesium, J. Colloid Interface Sci., 455 (2015) 39–45.
[8] X. Liu, G.R. Chen, D.J. Lee, T. Kawamoto, H. Tanaka, M.L. Chen, Y.K. Luo, Adsorption removal of cesium from drinking waters: a mini review on use of biosorbents and other adsorbents, Bioresour. Technol., 160 (2014) 142–149.
[9] M.A. Soliman, G.M. Rashad, M.R. Mahmoud, Fast and efficient cesium removal from simulated radioactive liquid waste by an isotope dilution-precipitate flotation process, Chem. Eng. J., 275 (2015) 342–350.
[10] S.M. Liu, H.H. Liu, Y.J. Huang, W.J. Yang, Solvent extraction of rubidium and cesium from salt lake brine with t-BAMBP-kerosene solution, Trans. Nonferrous. Met. Soc. China, 25 (2015) 329–334.
[11] S.J. Datta, W.K. Moon, D.Y. Choi, I.C. Hwang, K.B. Yoon, A novel vanadosilicate with hexadeca-coordinated Cs^+ ions as a highly effective Cs^+ remover, Angew. Chem. Int. Ed., 53 (2014) 7203–7208.
[12] D. Yang, S. Sarina, H. Zhu, H. Liu, Z. Zheng, M. Xie, S.V. Smith, S. Komarneni, Capture of radioactive cesium and iodide ions from water by using titanate nanofibers and nanotubes, Angew. Chem. Int. Ed., 50 (2011) 10594–10598.
[13] K.Y. Lee, M. Park, J. Kim, M. Oh, E.H. Lee, K.W. Kim, D.Y. Chung, J.K. Moon, Equilibrium, kinetic and thermodynamic study of cesium adsorption onto nanocrystalline mordenite from high-salt solution, Chemosphere, 150 (2016) 765–771.
[14] Y. Jiang, S.F. Shan, W. Liu, J. Zhu, Q.X. He, P. Tan, L. Cheng, X.Q. Liu, L.B. Sun, Rational design of thermo-responsive adsorbents: demand-oriented active sites for the adsorption of dyes, Chem. Commun., 53 (2017) 9538–9541.
[15] L. Cheng, Y. Jiang, N. Yan, S.F. Shan, X.Q. Liu, L.B. Sun, Smart adsorbents with photoregulated molecular gates for both selective adsorption and efficient regeneration, ACS Appl. Mater. Interfaces, 8 (2016) 23404–23411.
[16] Y. Jiang, P. Tan, L. Cheng, S.F. Shan, X.Q. Liu, L.B. Sun, Selective adsorption and efficient regeneration via smart adsorbents possessing thermo-controlled molecular switches, Phys. Chem. Chem. Phys., 18 (2016) 9883–9887.
[17] H. Yang, L. Sun, J. Zhai, H. Li, Y. Zhao, H. Yu, In situ controllable synthesis of magnetic Prussian blue/graphene oxide nanocomposites for removal of radioactive cesium in water, J. Mater. Chem. A, 2 (2014) 326–332.
[18] M. Ishizaki, S. Akiba, A. Ohtani, Y. Hoshi, K. Ono, M. Matsuba, T. Togashi, K. Kananizuka, M. Sakamoto, A. Takahashi, T. Kawamoto, H. Tanaka, M. Watanabe, M. Arisaka, T. Nankawa, M. Kurihara, Proton-exchange mechanism of specific Cs^+ adsorption via lattice defect sites of Prussian blue filled with coordination and crystallization water molecules, Dalton Trans., 42 (2013) 16049–16055.
[19] O.A.A. Moamen, H.A. Ibrahim, N. Abdelmonem, I.M. Ismailet, Thermodynamic analysis for the sorptive removal of cesium and strontium ions onto synthesized magnetic nano zeolite, Microporous Mesoporous Mater., 223 (2016) 187–195.
[20] T. Shibata, N. Seko, H. Amada, N. Kasai, S. Saiki, H. Hoshina, Y. Ueki, Evaluation of a cesium adsorbent grafted with ammonium 12-molybdophosphate, Radiat. Phys. Chem., 119 (2016) 247–252.
[21] M.R. Awual, Ring size dependent crown ether based mesoporous adsorbent for high cesium adsorption from wastewater, Chem. Eng. J., 303 (2016) 539–546.
[22] V.V. Milyutin, N.A. Nekrasova, N.Y. Yanicheva, G.O. Kalashnikova, Y.Y. Ganicheva, Sorption of cesium and strontium radionuclides onto crystalline alkali metal titanosilicates, Radiochemistry, 59 (2017) 65–69.
[23] Y. Wu, M. Hitoshi, N. Yuichi, O. Takashi, K. Shinichi, W.Y. Zhou, Study on adsorption behavior of cesium using ammonium tungstophosphate (AWP)-calcium alginate microcapsules, Sci. China Chem., 55 (2012) 1719–1725.
[24] H. Mimura, Y. Wu, W. Yufei, Y. Niibori, I. Yamagishi, M. Ozawa, T. Ohnishi, S. Koyama, Selective separation and recovery of cesium by ammonium tungstophosphate-alginate microcapsules, Nucl. Eng. Des., 241 (2011) 4750–4757.
[25] Y.K. Miura, H. Imai, T. Yokoi, T. Tatsumi, Y. Kamiya, Microporous cesium salts of tetravalent Keggin-type polyoxotungstates $Cs_4[SiW_{12}O_{40}]$, $Cs_4[PW_{11}O_{39}(Sn\text{-}n\text{-}C_4H_9)]$, and $Cs_4[PW_{11}O_{39}(Sn\text{-}OH)]$ and their adsorption properties, Microporous Mesoporous Mater., 174 (2013) 34–43.
[26] Y. Ogasawara, S. Uchida, T. Maruichi, R. Ishikawa, N. Shibata, Y. Ikuhara, N. Mizuno, Cubic cesium hydrogen silicododecatungstate with anisotropic morphology and polyoxometalate vacancies exhibiting selective water sorption and cation-exchange properties, Chem. Mater., 25 (2013) 905–911.
[27] F.P. Chen, G.P. Jin, S.Y. Peng, X.D. Liu, J.J. Tian, Recovery of cesium from residual salt lake brine in Qarham playa of Qaidam Basin with Prussian blue functionalized graphene/carbon fibers composite, Colloids Surf., A, 509 (2016) 359–366.
[28] J.Y. Su, G.P. Jin, T. Chen, X.D. Liu, C.N. Chen, J.J. Tian, The characterization and application of Prussian blue at graphene coated carbon fibers in a separated adsorption and electrically switched ion exchange desorption processes of cesium, Electrochim. Acta, 230 (2017) 399–406.
[29] B. Pangeni, H. Paudyal, K. Inoue, K. Ohto, H. Kawakita, S. Alam, Preparation of natural cation exchanger from persimmon waste and its application for the removal of cesium from water, Chem. Eng. J., 242 (2014) 109–116.
[30] H. Mimura, M. Saito, K. Akiba, Y. Onodera, Selective uptake of cesium by ammonium tungstophosphate (AWP)-calcium alginate composites, Solvent Extr. Ion Exch., 18 (2000) 1015–1027.